Key Engineering Materials
ISSN: 1662-9795, Vol. 926, pp 132-140
doi:10.4028/p-g078sc

Submitted: 2021-12-03
Revised: 2022-01-27
Accepted: 2022-02-18
Online: 2022-07-22

On the Influence of Cross-Section Size on Measured Strength of SLM-Produced AlSi10Mg-Alloy

Dmitry Vysochinskiy[1,a*], Naureen Akhtar [1,b]

[1*]University of Agder, Norway

[a*]dmitry.vysochinskiy@uia.no, [b]Naureen.Akhtar@uia.no

Keywords: Selective Laser Melting, AlSi10Mg, Tensile Test, Mechanical Properties, Surface Roughness, Size Effect, Metal 3D-printing, Microstructure

Abstract. The freedom in choice of geometries in additive manufacturing (AM) favors the use of structures with large surface and small cross-section such as lattice structures and thin-walled hollow profiles. On the other hand, the practices of strength testing of metals require a certain bulk of the material to be printed to be able to produce a sample and test material properties. The size of the sample cross section might influence the strength and up to 30% decrease in strength for small struts was reported in the literature. Understanding the influence of the cross-section size on the strength of SLM-produced metal is crucial to be able to relate the strength determined through tensile testing and the strength of an SLM-produced component with complex geometry. This article deals with effect of cross-section size on the measured strength of the SLM-produced AlSi10Mg-alloy. It is demonstrated how the decrease in strength can be explained by the difference between measured and actual cross-section area induced by surface roughness rather than by the difference in microstructure between the samples of different sizes.

Introduction

As the additive manufacturing (AM) technology develops beyond its initial niche of rapid prototyping towards the use of additively manufactured components as load bearing parts, the material testing engineers are faced with the need to characterize the strength and other mechanical properties of the AM-produced materials. Selective Laser Melting is a type of (AM) technology that allows to produce fully dense metal parts. This paper focuses on mechanical properties of AlSi10Mg, which is one of the most used SLM-processed aluminium alloys along with AlSi12 and AlSi7Mg.

Although, the mechanical properties of SLM-produced aluminum are extensively studied, lack of research based universally accepted guidelines and standards makes it is difficult to benchmark or compare the properties of the same material printed using different SLM-machines and/or different specimen geometries, as noted by [1]. ASTM F3122-14 [2] only provide some general guidelines on use of existing material testing standards on AM-products, but the existing standards are not fully adopted for additive manufacturing. E.g., when it comes to SLM produced aluminum, it is not clear how the rough surfaces produced by SLM-process should be handled, hence most researchers tend to machine their tensile samples, as Table 1 indicates. Studies that make direct comparison between different SLM-printers are scarce, among reviewed papers in Table 1, only one [3] makes a direct comparison of mechanical AlSi10Mg-alloy produced by different SLM-printers and a similar comparison was done by [4] for 316L austenitic steel. The comparison of different sample sizes and geometries also seems not to have received enough attention in the literature yet. In our earlier work we reported a comparison of strength of SLM-produced AlSi10Mg samples of different diameters [5]. Similar, but more focused study was reported by [6] who compared the strength, the microstructure and the porosity of AlSi10Mg samples of different diameters and reported up to 30% decrease in strength for small struts. [7] also studied size effect and made a comparison of microstructure of SLM-produced AlSi10Mg plates of different thickness, but no tensile properties were tested.

Table 1. Different uniaxial tension samples used for testing of SLM-produced aluminum

Tensile sample type and preparation methods	Publications
Machined cylindrical samples	[8]–[29]
Rectangular cross-section samples machined on all sides	[3], [30]–[35]
Flat cross-section samples cut out of a plate or thin-walled profile	[36]–[39]
Net shape rectangular cross-section samples that were sandblasted	[40]
Net shape cylindrical	[6], [41]–[43]
Mass-produced net shape rectangular samples	[44]

Understanding the influence of the sample cross-section size on the measured strength is crucial to be able to compare the values of strength reported using different sample geometries. In this article we complement our previous results from [5] with additional study of material microstructure and make a comparison with the results of [6] in order to gain a deeper understanding on how the measured strength and microstructure of SLM-produced AlSi10Mg are affected by the size of printed cross-section.

Materials and Methods

The experimental work reported in [5] and [45] includes 15 sets of uniaxial tension test samples printed in two rounds sets #1-6 in the first round and sets #7-15 in the second round. The samples were printed by SLM®280 metal printer with 400 W laser using 50 µm printing layer thickness and argon gas as protective atmosphere. AlSi10Mg powder for printing was acquired from TEKNA advanced material [46].

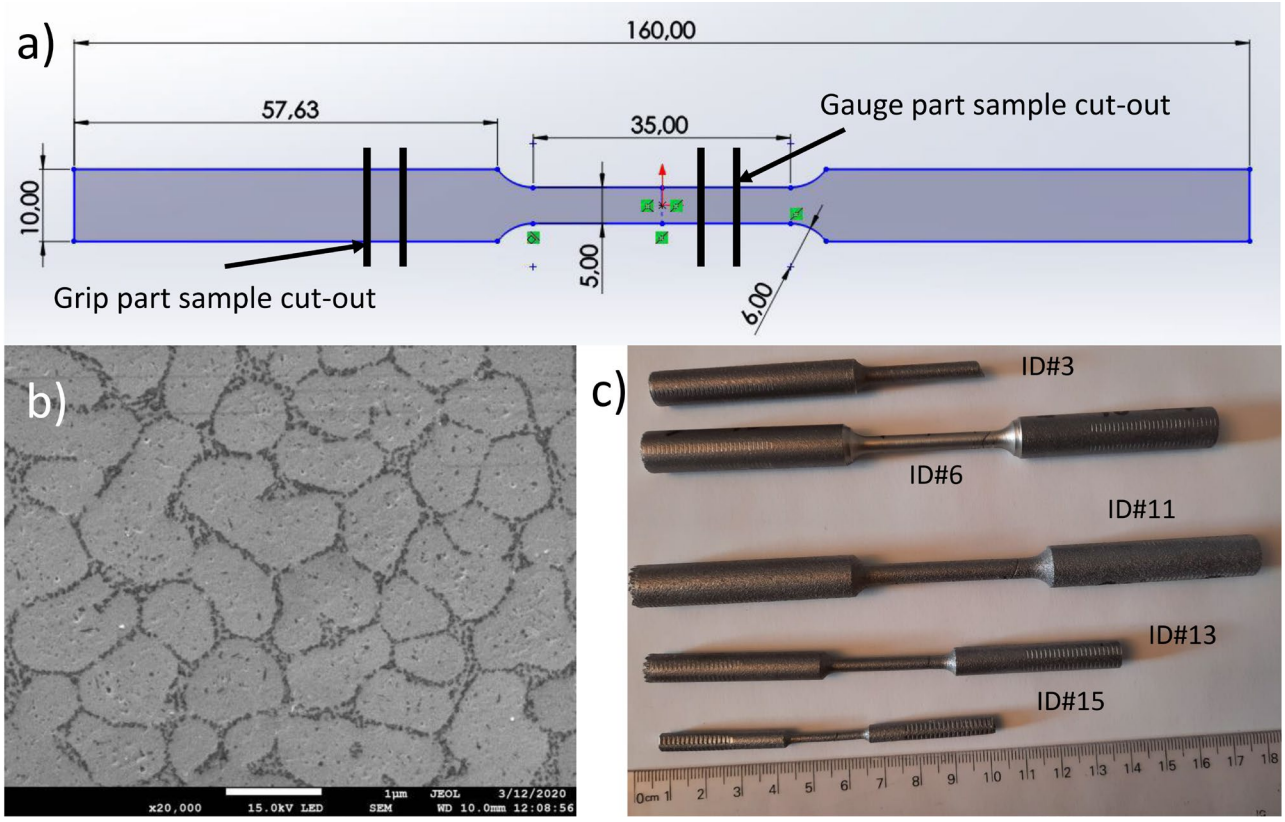

Fig. 1. Sample geometry (a), typical microstructure after printing (b) and samples of different diameters after testing (c)

Table 2. Selected tensile test series

Series ID	Yield strength [MPa]	Tensile strength [MPa]	Printed gauge part diameter [mm]	Printed grip part diameter [mm]	Tested sample diameter [mm]	Machined / Net shape	Printing round	Sample orientation
3	229.8±2.8	408.5±9.7	5.0	10.0	5.0	Net shape	1	Vertical
6	219.0±4.4	402.2±8.6	7.0	12.0	5.0	Machined	1	Vertical
11	209.8±1.3	381.6±7.6	2.5	5.0	2.5	Net shape	2	Vertical
13	212.8±2.8	414.8±8.6	4.0	8.0	4.0	Net shape	2	Vertical
15	221.2±9.9	397.3±12.9	6.0	12.0	6.0	Net shape	2	Vertical

This article aims at better understanding the effect of the sample size on measured strength of net shape samples; therefore, we concentrate on further analysis of series ID#3, ID#6, ID#11, ID#13, and ID#15 reported in Table 2. The samples in these series were oriented vertically i.e., in the build direction, which allows to 3D-print samples without the need for support structure. Overview of the all 15 series can be found in [5].

Cylindrical samples were used. Fig. 1a illustrates the geometry for d=5.0 mm sample; as can be seen, the parallel length L_c=35 mm, which allows for gauge length L_0=25 mm. Sample geometry is in accordance with [47]. Net shape samples were printed directly while the machined samples were printed with 1 mm surplus that was later machined away. Fig. 1c shows samples of different diameters; samples of 2.5 mm, 4.0 mm and 6.0 mm diameter were produced by scaling the original 5.0 mm diameter sample geometry.

The additional microstructure investigation reported in this article was performed using the Scanning Electron Microscope Jeol JSM-7200F. The samples for microstructure investigation were cut out of the gauge length section of the sample after the testing and from the grip part of the sample as Fig. 1a indicates.

Microstructure

The SLM-produced AlSi10Mg obtains a unique cellular microstructure shown in Fig. 1b, which forms due to rapid cooling and remelting during SLM-process. The microstructure is sub-granular i.e., the cells are substantially smaller that the individual grains (see e.g. [48] for EBSD images) and the cell walls consist of small particles of Si. The heat treatment or prolonged exposure to the heat under the printing process leads to formation of bigger spherical particles of Si in Al matrix and reduction of strength combined with increase of ductility.

[6] reported comparison of net shape AlSi10Mg samples with diameter in the gauge part d=5.0 mm, d=4.0 mm, d=3.0 mm, d=2.0 mm, and d=1.0 mm; they measured strength, microstructure, and porosity. [6] reported that sample strength decreases with diameter; porosity increases with diameter and the microstructure of the material varies in such a way that the silicon cell size decreases with diameter i.e., larger diameter leads to slightly larger average cell size.

Fig. 2 illustrates the microstructure of the samples with initial diameter in gauge area d=2.5 mm, 4.0 mm and 6.0 mm, the diameter of the grip area was twice as much i.e., 5.0 mm, 8.0 mm, and 12 mm, respectively. These three series were printed in the same printing round. Fig.2a-2c demonstrate microstructure of the gauge part of the sample, while Fig. 2d-2f demonstrate the microstructure of the grip part of the sample. It can be seen that the tendency described by [6] is present and the larger sample diameter generally shows larger cell size, but the tendency is not that well pronounced. Although, images shown in Fig. 2 are representative of most of the area in the corresponding samples, there are also areas with varied cell size within the same sample as shown in Fig. 3

The cell structure is slightly different close to the edge of the sample as Fig. 4 indicates; there are some elongated and open cells present. But no distinct difference in microstructure is observed between bulk and the edge material. Thus, study of microstructure didn’t show any unusual difference

between edge and bulk material that could have explained anomalous behavior of the machined samples from series ID6 discussed in [5].

Strength Variation with Sample Cross-Section

Fig. 5 presents the average yield strength and tensile strength of the sample series as function of the sample printed diameter. The strength of the machined samples from series ID#6 is placed at d=7.0 mm which corresponds to the printed cross-section diameter before machining. The strength values from [6] are also displayed for comparison. We can see that there is about 10% difference in yield strength between unmachined samples with d=2.5 mm and d=6.0 mm, the same goes for results reported by [6], where the difference in strength of d=2.0 mm and d=5.0 mm samples is about 10%.

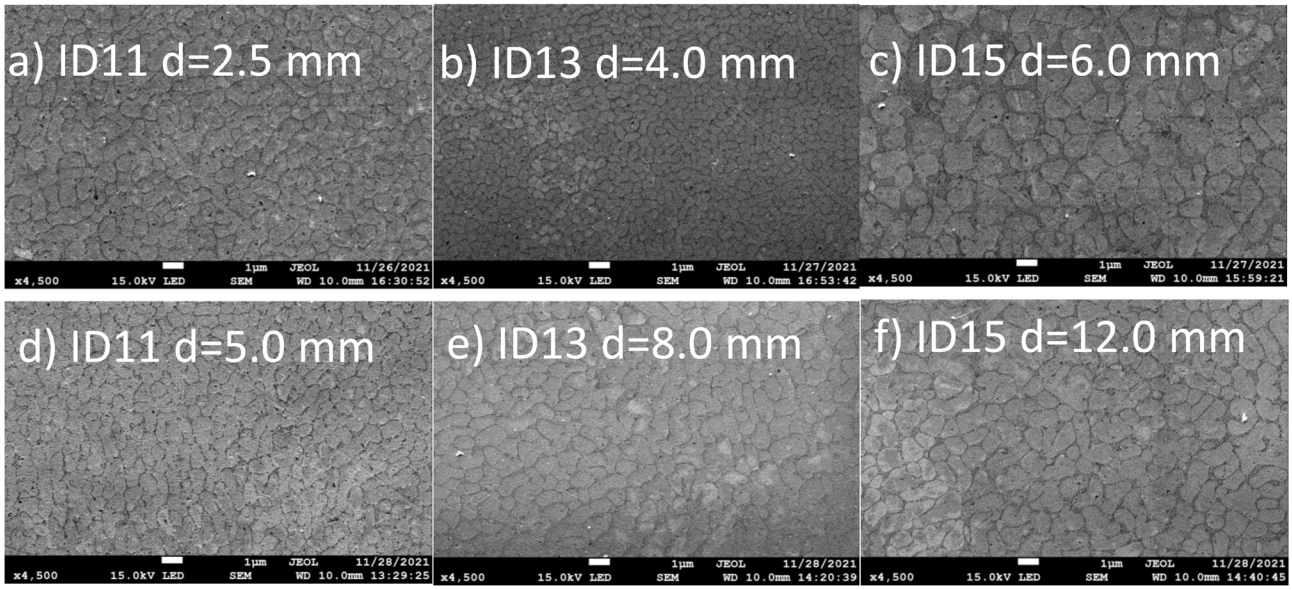

Fig. 2. Microstructure of gauge part and grip part of net shape samples

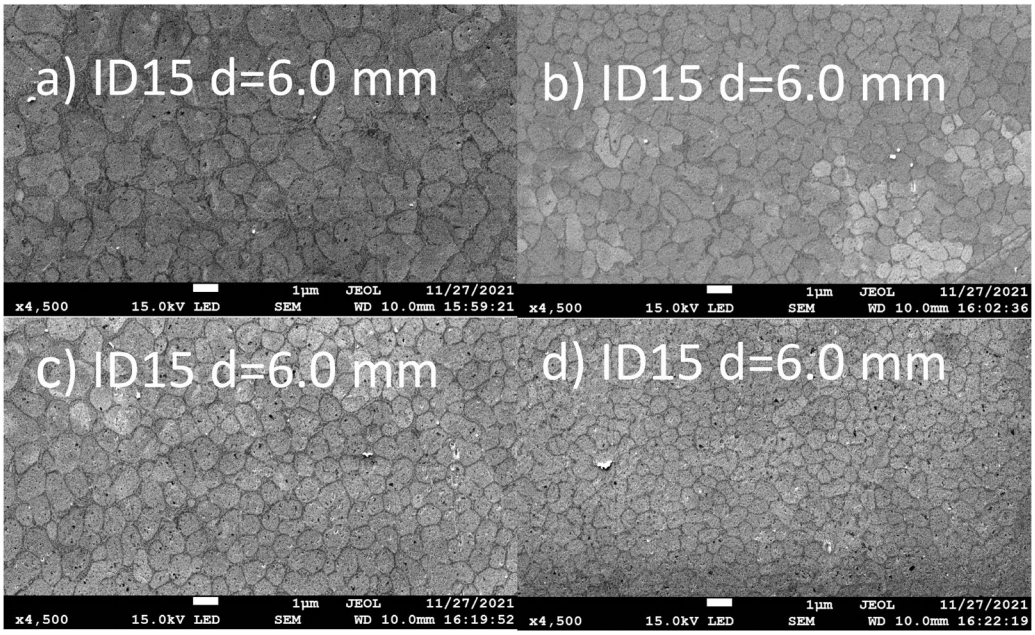

Fig. 3. Different cell sizes observed within the same sample

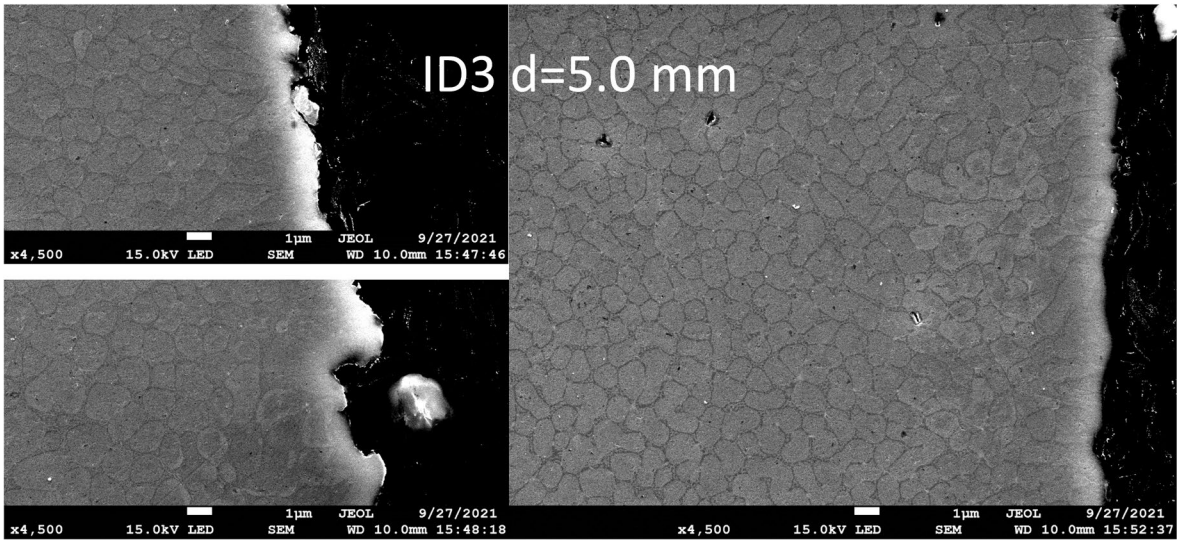

Fig. 4. Microstructure at the sample edge

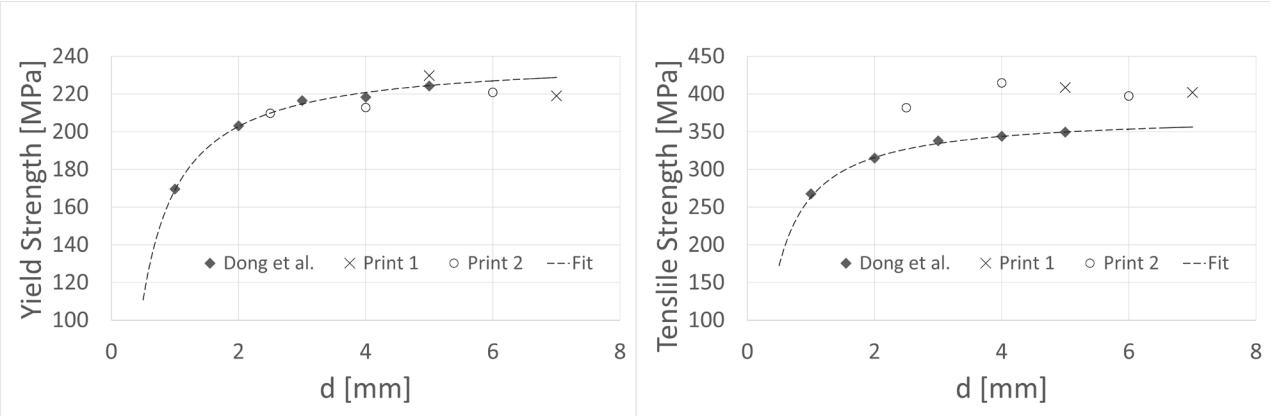

Fig. 5. Yield strength and Tensile Strength variation

There are three competing explanations for the different strength of the samples of different diameters displayed in Fig. 5. The possible explanations are the difference in microstructure, the different porosity, and the effect of surface roughness. Although the samples or struts with different diameter indeed display different microstructure when it comes to cell size, the different microstructure is an unlikely explanation for difference in strength. If the amount and size of the silicon particles that prevent dislocation motion remains the same, their distribution in form of the cell size is likely to have negligible effect on the yield strength. The porosity is also an unlikely candidate as the produced parts are dense. [6] report 1.87% porosity for the d=1mm samples, and 0.1% for d=5.0 mm samples. For the same samples, the difference in yield strength is about 10% between d=2.0 mm samples and d=5.0 mm and about 30% between d=1.0 mm and d=5.0 mm samples. This leaves the effect of surface roughness and the difference between measured or perceived area and the loaded cross-section area to be the most plausible explanation.

In case when the cross section has a rough surface, a natural approach for a structural analyst would be to try do define net cross section area i.e., the area that is actually involved in carrying the load. [49] explicitly suggested that the net dimensions of the cross section deviate from measured dimensions by the values of surface roughness and thus $2R_p$ need to be subtracted to determine the net dimensions for calculations of material strength, when dealing with unmachined AM-produced tensile samples. Using this approach, the connection between measured and actual engineering stress in the samples can be expressed as:

$$\sigma_{measured} = \sigma \frac{(d-2R_p)^2}{d^2} \tag{1}$$

Where $\sigma_{measured}$ is the engineering stress calculated using the uncorrected surface area, σ is the engineering stress determined using the reduced cross section area, d is initial diameter and the R_p is the reduction due to the surface roughness. Eq. 1 can be applied to both yield strength and tensile strength. Note that [49] suggest using the average peak roughness, but here we treat R_p simply as difference between the actual dimension and the measured one without getting into the discussion on how R_p should be measured or whether R_p represents actual surface roughness or is just a correction to represent the difference between measured and loaded cross-section dimensions.

Assuming the surface roughness correction R_p to be independent of diameter, we can fit the Eq. 1 to the measured yield strength data by selecting appropriate value of R_p. Eq. 1 fits well to our experimental results, but it is even better to fit it to result of [6] as displayed in Fig. 5 as there are more data points to utilize. The fit in Fig. 5 is set to go through the yield strength for the d=5.0 mm and the roughness correction R_p is set to fit the rest of the data, this gives $R_p = 0.16$ mm. The fit for tensile strength uses the same $R_p = 0.16$ mm and is only set to go through the tensile strength point of d=5.0 mm. Thus, we observe that the value of R_p determined to fit the variation in yield strength predicts the variation in tensile strength as well.

Discussion and Conclusions

One of the challenges that hinders a wider use of SLM products is variability of the mechanical properties of the produced parts. Hence, studying the influence of different parameters that might affect the properties of the produced alloy is vital for the further advance of applications of SLM-technology. AM opens for shape flexibility and allows to produce samples with cross-sections of different shapes and sizes and understanding how the measured material strength is influenced by the cross-section size is important to be able to compare the result form different studies. This paper studied how the size of the printed cross section affects the properties of the SLM-produced AlSi10Mg-alloy.

The tensile tests results are consistent with the earlier findings of [6], who reported 30% decrease in strength for d=1.0 mm samples in comparison with d=5.0 mm samples. However, while [6] tend to attribute the difference in strength to differences in microstructure, our microstructure investigation do not confirm that. Some minor difference in microstructure between samples with different printed cross-section area was observed, but this variation is not enough to explain observed difference in strength. Hence, an alternative explanation was provided. It was demonstrated that the difference in strength between samples of different diameters can be explained by the surface roughness causing a difference between measured and actually loaded cross-section area. The compensation for surface roughness not only explains the difference in strength between samples of different diameters, but also makes a correct prediction about strength of the small samples based on the strength of the large ones and correctly predicts variation in tensile strength based on variation in yield strength.

References

[1] P. Ponnusamy, R. A. R. Rashid, S. H. Masood, D. Ruan, and S. Palanisamy, “Mechanical properties of slm-printed aluminium alloys: A review,” *Materials (Basel).*, vol. 13, no. 19, pp. 1–51, Oct. 2020, doi: 10.3390/MA13194301.

[2] ASTM, *ASTM-F3122-14 Standard Guide for Evaluating Mechanical Properties of Metal Materials Made via Additive Manufacturing Processes 1*. 2014.

[3] A. T. Silvestri *et al.*, “Assessment of the Mechanical Properties of AlSi10Mg Parts Produced through Selective Laser Melting Under Different Conditions,” *Procedia Manuf.*, vol. 47, pp. 1058–1064, Jan. 2020, doi: 10.1016/J.PROMFG.2020.04.115.

[4] A. Röttger *et al.*, “Microstructure and mechanical properties of 316L austenitic stainless steel processed by different SLM devices,” *Int. J. Adv. Manuf. Technol. 2020 1083*, vol. 108, no. 3, pp. 769–783, Jul. 2020, doi: 10.1007/S00170-020-05371-1.

[5] D. Vysochinskiy, N. Akhtar, T. Nordmo, M. R. Strand, A. Vyssios, and M. K. Bak, "Experimental investigation of effect of printing direction and surface roughness on the mechanical properties of AlSi10Mg-alloy produced by selective laser melting," *Esaform 2021*, no. April, pp. 8–14, 2021, doi: 10.25518/esaform21.3627.

[6] Z. Dong, X. Zhang, W. Shi, H. Zhou, H. Lei, and J. Liang, "Study of Size Effect on Microstructure and Mechanical Properties of AlSi10Mg Samples Made by Selective Laser Melting," *Mater. 2018, Vol. 11, Page 2463*, vol. 11, no. 12, p. 2463, Dec. 2018, doi: 10.3390/MA11122463.

[7] N. Takata, H. Kodaira, A. Suzuki, and M. Kobashi, "Size dependence of microstructure of AlSi10Mg alloy fabricated by selective laser melting," *Mater. Charact.*, vol. 143, pp. 18–26, Sep. 2018, doi: 10.1016/J.MATCHAR.2017.11.052.

[8] N. T. Aboulkhair, I. Maskery, C. Tuck, I. Ashcroft, and N. M. Everitt, "The microstructure and mechanical properties of selectively laser melted AlSi10Mg: The effect of a conventional T6-like heat treatment," *Mater. Sci. Eng. A*, vol. 667, pp. 139–146, Jun. 2016, doi: 10.1016/j.msea.2016.04.092.

[9] A. Bin Anwar and Q. C. Pham, "Selective laser melting of AlSi10Mg: Effects of scan direction, part placement and inert gas flow velocity on tensile strength," *J. Mater. Process. Technol.*, vol. 240, pp. 388–396, Feb. 2017.

[10] B. J. Mfusi, N. R. Mathe, L. C. Tshabalala, and P. A. Popoola, "The Effect of Stress Relief on the Mechanical and Fatigue Properties of Additively Manufactured AlSi10Mg Parts," *Met. 2019, Vol. 9, Page 1216*, vol. 9, no. 11, p. 1216, Nov. 2019, doi: 10.3390/MET9111216.

[11] K. G. Prashanth, S. Scudino, and J. Eckert, "Defining the tensile properties of Al-12Si parts produced by selective laser melting," *Acta Mater.*, vol. 126, pp. 25–35, Mar. 2017, doi: 10.1016/J.ACTAMAT.2016.12.044.

[12] C. H. S. Rakesh, N. Priyanka, R. Jayaganthan, and N. J. Vasa, "Effect of build atmosphere on the mechanical properties of AlSi10Mg produced by selective laser melting," *Mater. Today Proc.*, vol. 5, no. 9, pp. 17231–17238, Jan. 2018, doi: 10.1016/J.MATPR.2018.04.133.

[13] H. Rao, S. Giet, K. Yang, X. Wu, and C. H. J. Davies, "The influence of processing parameters on aluminium alloy A357 manufactured by Selective Laser Melting," *Mater. Des.*, vol. 109, pp. 334–346, Nov. 2016, doi: 10.1016/J.MATDES.2016.07.009.

[14] R. Rashid *et al.*, "Effect of energy per layer on the anisotropy of selective laser melted AlSi12 aluminium alloy," *Addit. Manuf.*, vol. 22, pp. 426–439, Aug. 2018, doi: 10.1016/J.ADDMA.2018.05.040.

[15] I. Rosenthal, A. Stern, and N. Frage, "Microstructure and Mechanical Properties of AlSi10Mg Parts Produced by the Laser Beam Additive Manufacturing (AM) Technology," *Metallogr. Microstruct. Anal.*, vol. 3, no. 6, pp. 448–453, Dec. 2014, doi: 10.1007/S13632-014-0168-Y/FIGURES/10.

[16] I. Rosenthal, A. Stern, and N. Frage, "Strain rate sensitivity and fracture mechanism of AlSi10Mg parts produced by Selective Laser Melting," *Mater. Sci. Eng. A*, vol. 682, pp. 509–517, Jan. 2017, doi: 10.1016/j.msea.2016.11.070.

[17] S. Siddique, M. Awd, J. Tenkamp, and F. Walther, "High and very high cycle fatigue failure mechanisms in selective laser melted aluminum alloys," *J. Mater. Res.*, vol. 32, no. 23, pp. 4296–4304, Dec. 2017, doi: 10.1557/JMR.2017.314/TABLES/2.

[18] S. Siddique, M. Imran, E. Wycisk, C. Emmelmann, and F. Walther, "Influence of process-induced microstructure and imperfections on mechanical properties of AlSi12 processed by selective laser melting," *J. Mater. Process. Technol.*, vol. 221, pp. 205–213, Jul. 2015, doi: 10.1016/J.JMATPROTEC.2015.02.023.

[19] M. Tang, P. C. Pistorius, S. Narra, and J. L. Beuth, "Rapid Solidification: Selective Laser Melting of AlSi10Mg," *Springer*, doi: 10.1007/s11837-015-1763-3.

[20] A. Aversa *et al.*, "Effect of Process and Post-Process Conditions on the Mechanical Properties of an A357 Alloy Produced via Laser Powder Bed Fusion," *Met. 2017, Vol. 7, Page 68*, vol. 7, no. 2, p. 68, Feb. 2017, doi: 10.3390/MET7020068.

[21] U. Tradowsky, J. White, R. M. Ward, N. Read, W. Reimers, and M. M. Attallah, "Selective laser melting of AlSi10Mg: Influence of post-processing on the microstructural and tensile properties development," *Mater. Des.*, vol. 105, pp. 212–222, Sep. 2016, doi: 10.1016/J.MATDES.2016.05.066.

[22] N. E. Uzan, R. Shneck, O. Yeheskel, and N. Frage, "Fatigue of AlSi10Mg specimens fabricated by additive manufacturing selective laser melting (AM-SLM)," 2017, doi: 10.1016/j.msea.2017.08.027.

[23] M. Awd, F. Stern, A. Kampmann, D. Kotzem, J. Tenkamp, and F. Walther, "Microstructural Characterization of the Anisotropy and Cyclic Deformation Behavior of Selective Laser Melted AlSi10Mg Structures," *Met. 2018, Vol. 8, Page 825*, vol. 8, no. 10, p. 825, Oct. 2018, doi: 10.3390/MET8100825.

[24] R. Casati, M. H. Nasab, M. Coduri, V. Tirelli, and M. Vedani, "Effects of Platform Pre-Heating and Thermal-Treatment Strategies on Properties of AlSi10Mg Alloy Processed by Selective Laser Melting," *Met. 2018, Vol. 8, Page 954*, vol. 8, no. 11, p. 954, Nov. 2018, doi: 10.3390/MET8110954.

[25] L. Denti, "Additive Manufactured A357.0 Samples Using the Laser Powder Bed Fusion Technique: Shear and Tensile Performance," *Met. 2018, Vol. 8, Page 670*, vol. 8, no. 9, p. 670, Aug. 2018, doi: 10.3390/MET8090670.

[26] T. Kimura and T. Nakamoto, "Microstructures and mechanical properties of A356 (AlSi7Mg0.3) aluminum alloy fabricated by selective laser melting," *Mater. Des.*, vol. 89, pp. 1294–1301, Jan. 2016, doi: 10.1016/J.MATDES.2015.10.065.

[27] A. H. Maamoun, Y. F. Xue, M. A. Elbestawi, and S. C. Veldhuis, "The Effect of Selective Laser Melting Process Parameters on the Microstructure and Mechanical Properties of Al6061 and AlSi10Mg Alloys," *Mater. 2019, Vol. 12, Page 12*, vol. 12, no. 1, p. 12, Dec. 2018, doi: 10.3390/MA12010012.

[28] T. Maconachie *et al.*, "Effect of build orientation on the quasi-static and dynamic response of SLM AlSi10Mg," vol. 788, p. 139445, Jun. 2020, Accessed: Nov. 24, 2020. [Online]. Available: https://doi.org/10.1016/j.msea.2020.139445.

[29] I. Maskery *et al.*, "Fatigue Performance Enhancement of Selectively Laser Melted Aluminium Alloy by Heat Treatment," Aug. 2015.

[30] L. Y. Jiang *et al.*, "Preparation and mechanical properties of CNTs-AlSi10Mg composite fabricated via selective laser melting," *Mater. Sci. Eng. A*, vol. 734, pp. 171–177, Sep. 2018, doi: 10.1016/J.MSEA.2018.07.092.

[31] D.-K. Kim, J.-H. Hwang, E.-Y. Kim, Y.-U. Heo, W. Woo, and S.-H. Choi, "Evaluation of the stress-strain relationship of constituent phases in AlSi10Mg alloy produced by selective laser melting using crystal plasticity FEM," *J. Alloys Compd.*, vol. 714, pp. 687–697, 2017, doi: 10.1016/j.jallcom.2017.04.264.

[32] A. Majeed, M. Muzamil, J. Lv, B. Liu, and F. Ahmad, "Heat treatment influences densification and porosity of AlSi10Mg alloy thin-walled parts manufactured by selective laser melting technique," *J. Brazilian Soc. Mech. Sci. Eng. 2019 416*, vol. 41, no. 6, pp. 1–13, May 2019, doi: 10.1007/S40430-019-1769-9.

[33] P. Y. Sun, Z. K. Zhu, C. Y. Su, L. Lu, C. Y. Zhou, and X. H. He, "Experimental characterisation of mechanical behaviour for a TA2 welded joint using digital image correlation," *Opt. Lasers Eng.*, vol. 115, no. August 2018, pp. 161–171, 2019, doi: 10.1016/j.optlaseng.2018.11.022.

[34] N. Takata, H. Kodaira, K. Sekizawa, A. Suzuki, and M. Kobashi, "Change in microstructure of selectively laser melted AlSi10Mg alloy with heat treatments," *Mater. Sci. Eng. A*, vol. 704, pp. 218–228, Sep. 2017, doi: 10.1016/j.msea.2017.08.029.

[35] W. Li *et al.*, "Effect of heat treatment on AlSi10Mg alloy fabricated by selective laser melting: Microstructure evolution, mechanical properties and fracture mechanism," *Mater. Sci. Eng. A*, vol. 663, pp. 116–125, Apr. 2016, doi: 10.1016/j.msea.2016.03.088.

[36] T. Fiegl, M. Franke, and C. Körner, “Impact of build envelope on the properties of additive manufactured parts from AlSi10Mg,” *Opt. Laser Technol.*, vol. 111, pp. 51–57, Apr. 2019, doi: 10.1016/J.OPTLASTEC.2018.08.050.

[37] X. P. Li *et al.*, “A selective laser melting and solution heat treatment refined Al–12Si alloy with a controllable ultrafine eutectic microstructure and 25% tensile ductility,” *Acta Mater.*, vol. 95, pp. 74–82, Aug. 2015, doi: 10.1016/J.ACTAMAT.2015.05.017.

[38] J. Suryawanshi, K. G. Prashanth, S. Scudino, J. Eckert, O. Prakash, and U. Ramamurty, “Simultaneous enhancements of strength and toughness in an Al-12Si alloy synthesized using selective laser melting,” *Acta Mater.*, vol. 115, pp. 285–294, Aug. 2016, doi: 10.1016/J.ACTAMAT.2016.06.009.

[39] M. Costas, D. Morin, M. de Lucio, and M. Langseth, “Testing and simulation of additively manufactured AlSi10Mg components under quasi-static loading,” *Eur. J. Mech. A/Solids*, vol. 81, p. 103966, May 2020, doi: 10.1016/j.euromechsol.2020.103966.

[40] R. Subbiah, J. Bensingh, A. Kader, and S. Nayak, “Influence of printing parameters on structures, mechanical properties and surface characterization of aluminium alloy manufactured using selective laser melting,” *Int. J. Adv. Manuf. Technol.*, vol. 106, no. 11–12, pp. 5137–5147, Feb. 2020, doi: 10.1007/S00170-020-04929-3/FIGURES/11.

[41] M. Fousová, D. Dvorský, A. Michalcová, and D. Vojtěch, “Changes in the microstructure and mechanical properties of additively manufactured AlSi10Mg alloy after exposure to elevated temperatures,” *Mater. Charact.*, vol. 137, pp. 119–126, Mar. 2018, doi: 10.1016/j.matchar.2018.01.028.

[42] A. Iturrioz, E. Gil, M. M. Petite, F. Garciandia, A. M. Mancisidor, and M. San Sebastian, “Selective laser melting of AlSi10Mg alloy: influence of heat treatment condition on mechanical properties and microstructure,” *Weld. World 2018 624*, vol. 62, no. 4, pp. 885–892, Apr. 2018, doi: 10.1007/S40194-018-0592-8.

[43] A. Pola *et al.*, “Evaluation on the fatigue behavior of sand-blasted AlSi10Mg obtained by DMLS,” *Frat. ed Integrità Strutt.*, vol. 13, no. 49, pp. 775–790, Jun. 2019, doi: 10.3221/IGF-ESIS.49.69.

[44] C. M. Laursen, S. A. DeJong, S. M. Dickens, A. N. Exil, D. F. Susan, and J. D. Carroll, “Relationship between ductility and the porosity of additively manufactured AlSi10Mg,” *Mater. Sci. Eng. A*, vol. 795, p. 139922, Sep. 2020, doi: 10.1016/J.MSEA.2020.139922.

[45] T. Nordmo, M. R. Strand, and A. Vyssios, “Mekaniske egenskaper til selektiv lasersmeltet AlSi10Mg-legering,” University of Agder, 2020. Accessed: Nov. 24, 2020. [Online]. Available: https://uia.brage.unit.no/uia-xmlui/handle/11250/2679275.

[46] “AlSiMg Aluminum Alloy Spherical Powder | Tekna.” http://www.tekna.com/spherical-powders/alsimg_aluminum_alloy (accessed Nov. 27, 2020).

[47] *Metalliske materialer : strekkprøving = Metallic materials : tensile testing : part 1 : Method of test at room temperature (ISO 6892-1:2016) : Del 1 : meode for prøving ved romtemperatur (ISO 6892-1:2016)*, vol. NS-EN ISO. Lysaker: Standard Norge, 2016.

[48] N. T. Aboulkhair, M. Simonelli, L. Parry, I. Ashcroft, C. Tuck, and R. Hague, “3D printing of Aluminium alloys: Additive Manufacturing of Aluminium alloys using selective laser melting,” *Prog. Mater. Sci.*, vol. 106, p. 100578, Dec. 2019, doi: 10.1016/J.PMATSCI.2019.100578.

[49] B. C. Salzbrenner *et al.*, “High-throughput stochastic tensile performance of additively manufactured stainless steel,” *J. Mater. Process. Technol.*, vol. 241, pp. 1–12, Mar. 2017, doi: 10.1016/j.jmatprotec.2016.10.023.